MICROMECHANICS-BASED MODELLING OF DUCTILE TEARING IN THIN PLATES

F. Hachez[1], A. G. Atkins[2], R.H. Dodds[3], T. Pardoen[1]

[1]Département des Sciences des Matériaux et des Procédés, Université catholique de Louvain, IMAP, Place Sainte Barbe 2, B-1348, Louvain-la-Neuve, Belgium (pardoen@pcim.ucl.ac.be)
[2]Department of Engineering, University of Reading, PO Box 225, Whiteknights, Reading RG6 2AY, U.K. (a.g.atkins@reading.ac.uk)
[3]Department of Civil and Environmental Engineering, University of Illinois, 2129 Newmark Lab, 205 North Mathews Avenue, Urbana, IL 61801-2397, USA (rdodds@uiuc.edu)

Abstract

Fracture tests performed on a large number of thin metal sheets with moderate to high hardening capacity systematically exhibit (i) mode I “cup & cup” fracture profiles with limited or no shear lips and significant localized necking, (ii) a fracture toughness that linearly increases with increasing thickness. In thin plates, the development of a localized neck in front of the crack tip indeed contributes to fracture toughness and leads to a thickness dependence. The total work of fracture Γ can be separated in three different terms: $\Gamma = \Gamma_0 + \Gamma_n + \Gamma_p$, where Γ_0 is the "intrinsic" fracture toughness accounting for damage and material separation, Γ_n is the work per unit crack advance required for localized necking, and Γ_p is the extrinsic contribution resulting from gross plastic dissipation during crack propagation. Depending on the microstructure of the material, the flow properties and the geometry, either the necking work or the fracture energy can dominate and the resulting thickness effect can be either very large or insignificant.

Introduction

The perceived wisdom about thin sheet fracture is that (i) the crack propagates under mixed mode I & III giving rise to a slant through-thickness fracture profile and (ii) the fracture toughness remains constant at low thickness and eventually decreases with increasing thickness. In the present study, fracture tests performed on thin DENT plates of various thicknesses made of stainless steel, 6082-O and NS4 aluminium alloy, brass, bronze, lead, and zinc systematically exhibit (i) *mode I* "bath-tub", i.e. "cup & cup", fracture profiles with limited shear lips and significant localized necking, (ii) a fracture toughness that *increases* with increasing thickness (in the range of 0.5 to 5 mm). The goals of the paper are

- to report about the experimental campaign;
- to validate and describe the trends obtained with two separate models, one for the necking contribution Γ_n and one for the fracture contribution Γ_0 for various material parameters and plate thickness;
- to combine the two models in order to explain their relationship and the reason for the thickness effect.

Experimental results

Mechanical tests All the materials were tested under uniaxial tension using dog-bone shaped rectangular specimens. The plastic response was systematically fitted by:

$$\frac{\bar{\sigma}}{\sigma_0} = \left(1 + k\bar{\varepsilon}^p\right)^n \tag{1}$$

where, $\bar{\sigma}$ is the effective stress, $\bar{\varepsilon}^p$ is the effective plastic strain, σ_0 is the yield stress, n is the strain hardening exponent and k is a parameter that is usually much larger than 1. The materials are listed in Table 1 with their mechanical properties.

Table 1. Material properties: E is the Young's modulus, σ_0 is the yield stress, k and n are the parameters in relation (1), obtained by a power law fit on the uniaxial stress strain curve, r_f is the thickness reduction factor defined by Eq. (4), X_0 is the mean initial void spacing (* mean grain size for Zn), Γ_0 is true work of fracture and w_n is the work of necking per unit volume.

Materials	E (GPa)	σ_0 (MPa)	n	k	r_f	X_0 (μm)	w_n^{exp} (MJ/m^3)	w_n^{model} (MJ/m^3)	Γ_0^{exp} (kJ/m^2)	Γ_0^{model} (kJ/m^2)
Steel A316L	210	310	0.48	25	0.48	25-50	204	165	221	172-345
Al 6082-O	70	50	0.26	265	0.6	10-20	33	32	28	8-16
Brass A	110	100	0.6	33	0.78	5-10	161	195	87	108-217
Al NS4 // RD	70	140	0.17	159	0.8	8-15	42	39	51	26-48
Zinc // RD	61	100	0.15	118	0.59	25*	64	23	34	16.5
Lead	16	7	0.25	290	1		7.3	5.3	0	0
Bronze A	100	120	0.51	38	0.7	4-5	218	166	70	51-63

The DENT geometry shown in Fig. 1 was chosen because of the simplifications resulting from the symmetry and from the confinement of the plastic zone in the ligament when the cracks are long enough. For dimensional reasons, the work of necking per unit area scales with the plate thickness while the work of diffuse plasticity scales with the ligament length. The total work W_t thus can be written

$$W_t = \Gamma_0 L_0 t_0 + w_n \alpha t_0^2 L_0 + w_p \beta t_0 L_0^2 \tag{2}$$

where t_0 is the initial plate thickness, L_0 is the initial ligament length, α and β are shape factors, w_n is the average work per unit volume dissipated in the neck in front of the crack tip and w_p is the average work per unit volume spent in plasticity in the diffuse plastic zone. By measuring the total energy W_t for separating a DENT specimen for different thicknesses and ligament lengths and by dividing this energy by the ligament area ($\Gamma = W_t/L_0 t_0$), it is thus possible to separate Γ_0, w_n and w_p:

$$\Gamma = \Gamma_0 + w_n \alpha t_0 + w_p \beta L_0 \,. \tag{3}$$

This idea extends the essential work of fracture method proposed by Cotterell and Reddel [1]. The values of the work of fracture Γ_0 and w_n of the different materials tested in this study are given in Table 1. The fracture work Γ_0 values range from 0 in lead to more than 200 kJ/m^2 in stainless steel. Both the necking and damage contributions are important in the fracture of ductile thin plates in the 1 mm-range of thickness.

Fractographic analyses (a) All materials exhibit a "cup & cup" or "bath-tub" fracture profile sketched in Fig. 2: the shape of the two matching fracture surfaces is similar. A regular fracture surface with dimples is observed along the sides of the specimen without any evidence of the shear distortion typical of fracture surfaces resulting from shear failure. As represented in Fig. 2, the mode I bath-tub fracture profile can be explained by the difference of stress triaxiality between the centre and the sides of the specimens. The surface is in a pure plane stress state involving thus a fracture strain larger than in the centre where the stress triaxiality has been increased due to necking stress concentration.

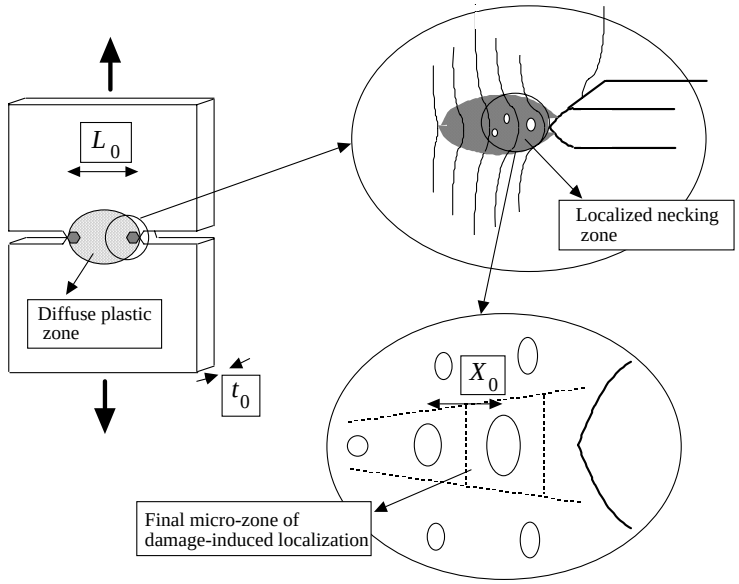

FIGURE 1. The DENT geometry with the diffuse and localized plastic zones (macro-scale), the localized necking zone (meso-scale) and the true fracture zone with the void spacing definition (micro-scale)

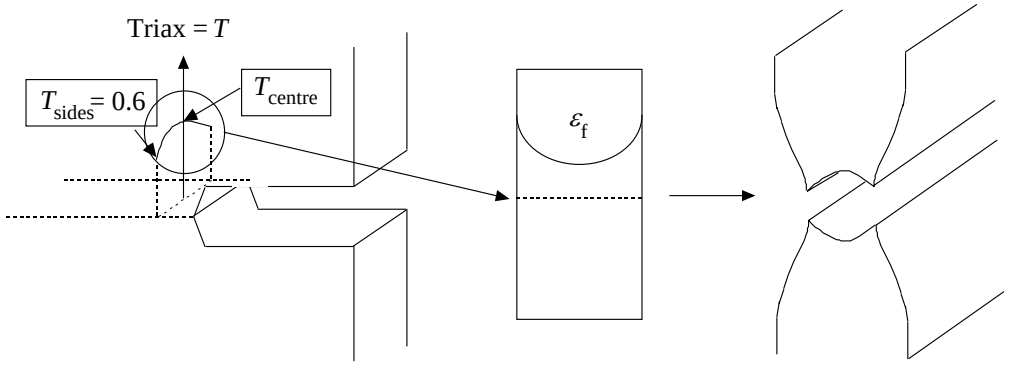

FIGURE 2. Bath-tub fracture profile (or "cup & cup") resulting from a higher stress triaxiality and thus lower fracture strain in the centre of the plate

(b) The thickness reduction factor r_f, defined as

$$r_f = \frac{t_0 - t_f}{t_0} \tag{4}$$

where t_f is the final plate thickness of the fracture plane in the neck, has been measured on micrographs taken from the top view (see Table 1). As no systematic dependence of r_f on thickness is observed, the r_f values are averaged over the different thicknesses. It is interesting also to point out again the behaviour of lead which fails by full necking, i.e. without any apparent damage mechanism. For the other materials, the reduction of thickness is always larger than about 50%.

(c) The fracture surfaces have been observed by SEM in order to characterize the micro-mechanisms of fracture, and to estimate the dimple sizes and spacing. The spacing has been quantified in the direction of crack advance which, owing to the near plane strain conditions, gives a direct image of the initial defect spacing, X_0, see Table 1.

More details about this experimental campaign can be found in Pardoen *et al.* [2].

Model 1 - work of necking

Dimensional analysis shows that, for a material with a flow behaviour represented by (1) and for a given geometry and stress state, the average work per unit volume w_n spent in the neck can be expressed as

$$\frac{w_n}{\sigma_0} = F\left[n, k, \frac{\sigma_0}{E}, \nu, \varepsilon_f\right], \tag{5}$$

where ε_f is the strain at fracture. In Pardoen *et al.* [2], a model has been proposed to evaluate (5) assuming plane strain tension stress state, see Hill [3]. The model is closed-form except for the evaluation of the shape parameter of the necking region whose adjustment has required conventional FE simulations. For a given geometry and loading configuration, this shape factor only depends on the strain hardening exponent *n*.

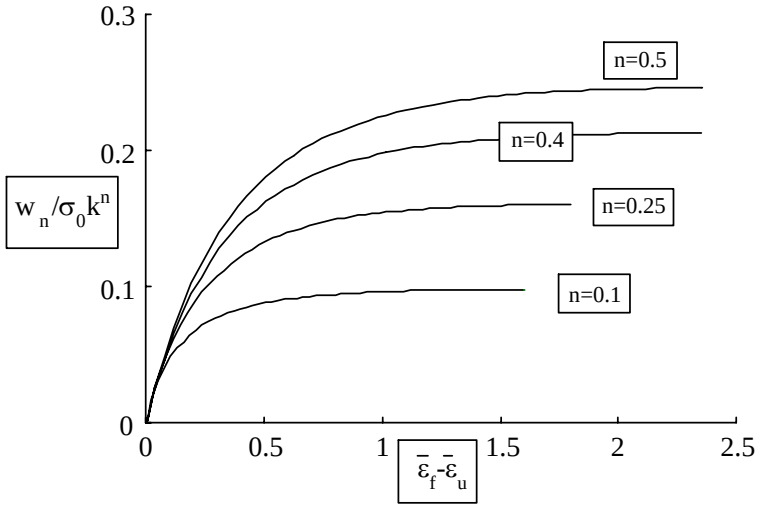

FIGURE 3. Variation of the average work of necking (per unit volume) as a function of the fracture strain minus the necking strain.

Fig. 3 shows the variation of $w_n/\sigma_0 k^n = \Gamma_n/\sigma_0 k^n t_0$ as a function of the equivalent strain at fracture $\bar{\varepsilon}_f$ minus the equivalent necking strain $\bar{\varepsilon}_u$ for different *n*. The work of necking per unit volume levels out at high fracture strains as the active necking zone becomes

increasingly small, involving increasingly less additional plastic work. The important factor for the necking contribution is not the fracture strain but the difference between the strain at necking and the fracture strain. In order to compare the model and the experiments, the reduction of thickness r_f was transposed into an equivalent fracture strain. The comparison between the experimental and predicted values of w_n is provided in Table 1. The agreement is very good except for zinc. The main reason for this discrepancy obviously comes from significant plastic anisotropy of zinc while the model relies on isotropic J2 plasticity.

Using the previous analysis, it is possible to separate Γ_0 and w_n from a test performed on a single thickness specimen. This procedure is especially useful if the same material has to be used in an application where the thickness has to be changed, for instance by machining, or where the thickness is not constant. Also this procedure allows comparison of different materials with different as-processed thicknesses without requiring the machining of specimens at the same thickness.

Model 2 - work of fracture

The model presented in this section aims at relating the energy Γ_0 spent for the growth and coalescence of voids in the localized neck to the microstructure of the metal. The evaluation of Γ_0 is of course very complex. Even in the case of idealized microstructure, most models existing in the literature remain essentially qualitative regarding the prediction of absolute values of the fracture toughness from the microstructure without parameter tuning or calibration. As depicted in Fig. 1, we assume a material made of regularly distributed voids (the voids are supposed to be present from the beginning of the loading) with initial spacing X_0 and initial volume fraction f_0. Only voids that are initially spherical will be considered. Dimensional analysis shows that for a material containing a uniform distribution of spherical voids and plastic flow properties given by (1) the fracture energy Γ_0 can be expressed as

$$\frac{\Gamma_0}{\sigma_0 X_0} = F\left(n, \frac{\sigma_0}{E}, k, \nu, f_0\right). \tag{6}$$

In thin plates, voids are subjected to a low stress triaxiality even in the localized neck in front of the propagating crack. Low stress triaxiality is much more difficult to handle when modelling ductile fracture than large stress triaxiality as it involves significant void shape changes (e.g. Budiansky *et al.* [4]). The elongation of the void in the direction of the maximum principal load not only reduces the void growth rate with respect to the rate of growth of a spherical void but also significantly delays the onset of coalescence. For that reason, use has been made of an extended version of the Gurson model developed by Pardoen and Hutchinson [5,6] which accounts for void shape effects on both the void growth and void coalescence processes. This constitutive model has been implemented in the finite element program ABAQUS through a User defined MATerial subroutine.

As for the necking problem, the complex 3D stress state existing at the crack tip will be approximated in order to simplify the analysis by plane strain tension allowing for necking development. The 2D finite strain simulations have been performed using the UMAT mentioned above for the constitutive material response. Γ_0 is evaluated in the most loaded element, i.e. the element located in the centre of the minimum section of the neck, from the calculated stress displacement response (see ref [2] for more details).

The model has been validated in the following way. The initial void volume fraction f_0 was identified by simulating the uniaxial tensile tests and finding the value that allows reproducing the experimental fracture strains. The void spacing X_0 measured experimentally (see Table 1) have been used to estimate Γ_0. The experimental and predicted Γ_0 are compared in Table 1. Although all these results remain semi-quantitative due to the numerous approximations in the model and the experimental uncertainty, it can be concluded

that, considering the wide range of materials tested, the results are very satisfactory and that the model captures the main features characterizing damage evolution in thin metal plates.

For a given geometry, loading configuration and a constant product $\sigma_0 X_0$, the two most important parameters affecting ductile fracture, i.e. affecting the non-dimensional function F in (6), are the initial void volume fraction f_0 and the strain-hardening exponent n. The other parameters that have been kept constant are : $\sigma_0/E = 1/k = 10^{-3}$, $\nu = 0.3$. Fig. 4 presents the variation of $\Gamma_0/X_0\sigma_0$ as a function of f_0 for n equal to 0.1, 0.3 and 0.5. The effect of both n and f_0 is obvious: large n and low f_0 significantly increase Γ_0.

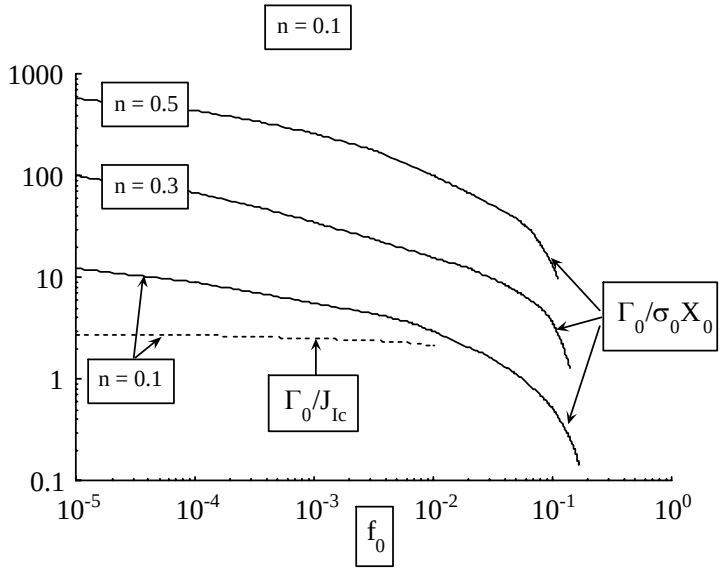

FIGURE 4. Variation of the predicted fracture energy as a function of the initial porosity for different strain hardening exponent; variation of the ratio of the plane stress fracture energy over the plane strain fracture toughness as a function of the initial porosity.

The "plane stress fracture energy" Γ_0 is also compared to the plane strain fracture toughness J_{Ic} in Fig. 4. For that purpose, the results obtained in ref [6] giving $J_{Ic}/X_0\sigma_0$ as a function of f_0 for the 2D, plane strain, small scale yielding, boundary value problem, were used to evaluate the ratio Γ_0/J_{Ic} for $n = 0.1$. To a first approximation the ratio Γ_0/J_{Ic} is not significantly affected by the initial porosity, nor by the value of the strain hardening exponent (result not shown). It ranges between 2.5 and 3.5 which agrees very well with full 3D FE modelling of crack propagation in thin and thick HSLA steel plates recently reported by Rivalin *et al.* [7]. The plane stress fracture energy is significantly larger than the plane strain value because of the much smaller stress triaxiality, which involves smaller void growth rate. To our knowledge, there exist no non-controversial experimental data in the literature to assess this prediction. The difficulty is to find a material which will be (a) ductile enough to show the necking mechanism at small thickness but (b) not so ductile that the thickness of the plane strain specimen will be excessively large.

At this point, with the models developed in the two previous sections, it is possible to come back to the problem of the coupling between crack tip necking and crack tip damage. Fig. 5 gathers the results of Figs 3 and 4 in terms of the variation of the ratio $\Gamma_0 X_0 k^n/\Gamma_n t_0$ as a function of f_0. The proportion of damage and necking contributions in the work of fracture depends very much on n and f_0 and linearly scales with X_0/t_0. Fig. 5 exhibits two limits: one when $f_0 \rightarrow$ 0.1-0.2 and one when $f_0 \rightarrow 0$. The first limit corresponds to highly porous materials where the fracture strain becomes smaller than the necking strain and thus Γ_n is equal to 0. This limit is attained for very large initial porosity (>0.1) that is not encountered

in typical industrial alloys. The other limit when $f_0 \rightarrow 0$ also leads to fracture toughness that is mainly controlled by the damage mechanisms, because Γ_n then saturates at large fracture strains (see Fig. 3). However, this limit is not really meaningful as our model is no longer valid when f_0 tends to zero and thus X_0 goes to infinity in finite specimens. Indeed, the thickness of the plate sets a second length scale. Thus the real limit for $f_0 \rightarrow 0$, which probably corresponds to experimental results for lead, is that Γ_0 tends to 0 and that fracture is then only controlled by plastic necking. In between these two limits, a local minimum appears over the range of porosity. This minimum corresponds to the maximum amount of necking dissipation with respect to damage.

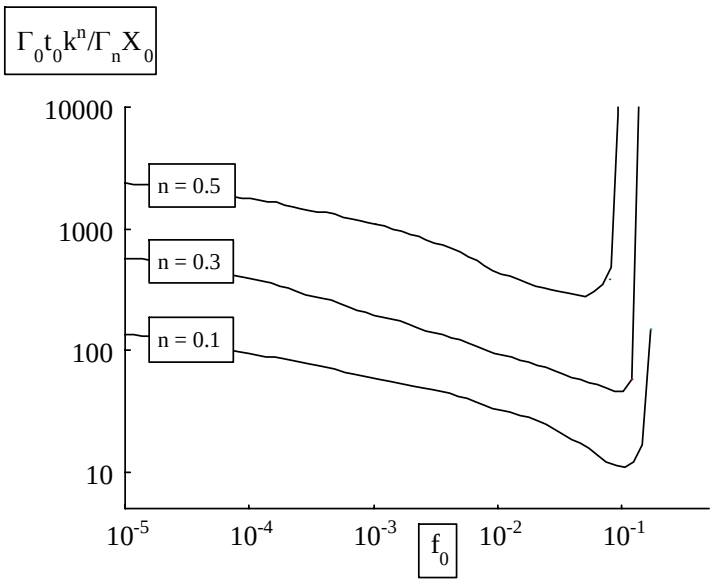

FIGURE 5. Variation of the ratio of the fracture and the necking work as a function of the initial porosity for different strain hardening exponent.

Fig. 5 also shows the marked effect of the strain hardening capacity on the energy partitioning. Increasing the hardening capacity affects much more the fracture contribution than the necking contribution for a given ratio X_0/t_0. The wide variety of behaviours that can be deduced from Fig. 5 probably explains the wide variations of apparent properties encountered in thin plates and the difficulty of rationalizing experimental measurements from only a macroscopic point of view (e.g. Broek [9]). It is interesting to consider two extreme, but realistic, cases:

1. Let us consider a low hardening (n = 0.1), highly porous ($f_0 = 3\text{x}10^{-2}$) material (e.g. Al alloys sometimes show large initial void volume fraction in that range) with a small ratio X_0/t_0 = 1/200 (e.g. X_0 = 5 μm, t_0 = 1 mm). From Fig. 5, Γ_0/Γ_n is equal to about 1/10. In such a material, the fracture toughness is essentially given by the necking contribution (although fracture is of course still controlled by the damage mechanisms and by Γ_0) and the fracture toughness is expected to markedly increase with thickness (while remaining in the quasi plane stress regime). It is thus not surprizing that the Γ_0 contribution has not been detected in some materials (e.g. Powell and Mai [8]).

2. Let us consider a high hardening (n = 0.5), low porosity ($f_0 = 10^{-4}$) material with a high ratio X_0/t_0 = 1/20 (e.g. X_0 = 50 μm, t_0 = 1 mm). From Fig. 5, Γ_0/Γ_n is equal to about 100. In such a material, the fracture toughness is essentially given by the fracture contribution and the fracture toughness is not expected to significantly increase with thickness. In fact, we believe that a decrease of the toughness with increasing thickness will be measured in such

materials. Indeed, Γ_0 is affected by the stress state. With increasing thickness, stress triaxiality will tend to increase at the crack tip, to accelerate the void growth rate with respect to the plane strain tension situation, to decrease the fracture strain and thus to lead to a decrease of Γ_0. This can justify results (e.g. Broek [9]) where the toughness is observed to always decrease with increasing thickness even at small thicknesses.

Conclusions

This study shows that slant fracture may be the exception rather than the rule. Thin plate fracture has been investigated mostly on high strength aluminium alloys or high strength steels which exhibit the slant fracture mode probably because of a relatively low hardening capacity and small fracture strain. The present work does not lead to quantitative data or to a criterion for solving the problem of the competition between shear localisation and slant fracture with respect to mode I fracture with necking. Nevertheless, this work suggests that slant fracture is avoided when the fracture strain is large enough to allow significant necking development before cracking initiation. If necking has not developed enough, the crack is not constrained to remain in the plane of the ligament and can tilt at 45°.

The work of necking (per unit area) (i) scales linearly with thickness, (ii) depends on the hardening exponent, and (iii) increases with the fracture strain to reach a constant value at large fracture strains. The work of fracture (per unit area) scales linearly with the yield stress and void spacing, and strongly depends on the initial porosity and hardening exponent. All combinations are possible: a small or large necking contribution associated with small or large fracture contribution. A large fracture term coupled with a small necking contribution will not lead to significant thickness effects in the quasi-plane stress regime while the opposite will be observed when necking dominates.

The analysis proposed in this paper is valid only (1) in the low stress triaxiality regime typical of thin sheets tearing and (2) for the steady state crack propagation. Only full 3D calculations are capable of describing either the transient or to encompass both thin and thick sheets, as well as to better capture the competition with the slant fracture mode. Promising preliminary results have been obtained with the extended Gurson model or with 3D cohesive zone models with parameters motivated by the present study.

Acknowledgements Fruitful discussions with J. Besson and A. Pineau (Ecole des Mines de Paris, Centre des Matériaux), B. Cotterell (University of Sydney and IMRE Singapore), F. Delannay (Université catholique de Louvain), J.W. Hutchinson (Harvard University) are gratefully acknowledged. The work of F. Hachez has been supported by a fellowship from FNRS, Belgium.

References

1. Cotterell, B., Reddel, J.K., *Int. J. Fract.*, vol **13**, 267-277, 1977
2. Pardoen, T., Hachez, F., Marchioni, B., Blyth, P.H. and Atkins, A.G., *J. Mech. Phys. Solids*, vol. **52**, 423-452, 2004
3. Hill, R., *J. Mech. Phys. Solids*, vol **1**, 19-30, 1952
4. Budiansky, B., Hutchinson, J.W., and Slutsky, S., In *Mechanics of Solids, The Rodney Hill 60th Anniversary Volume*, edited by H.G. Hopkins and M.J. Sewell, Pergamon Press, 1982, 13-45
5. Pardoen, T., Hutchinson, J.W., *J. Mech. Phys. Solids*, vol **48**, 2467-2512, 2000
6. Pardoen, T., Hutchinson, J.W., *Acta Mater.*, vol **51**, 133-148, 2003
7. Rivalin, F., Besson, J., Pineau, A., and Di Fant, M., *Engng. Fract. Mech.*, vol **68**, 347-364, 2001
8. Mai, Y.W., Powell, P., *J. Polymer Sc. B.*, vol **29**, 785-793, 1991
9. Broek, D., *Elementary fracture mechanics*, Nijhof, 1986